Video Article

A Paired Bead and Magnet Array for Molding Microwells with Variable Concave Geometries

Gi-Hun Lee[1], Youngjoon Suh[1], Joong Yull Park[1]

[1]School of Mechanical Engineering, College of Engineering, Chung-Ang University

Correspondence to: Joong Yull Park at jrpark@cau.ac.kr

Abstract

A spheroid culture is a useful tool for understanding cellular behavior in that it provides an *in vivo*-like three-dimensional environment. Various spheroid production methods such as non-adhesive surfaces, spinner flasks, hanging drops, and microwells have been used in studies of cell-to-cell interaction, immune-activation, drug screening, stem cell differentiation, and organoid generation. Among these methods, microwells with a three-dimensional concave geometry have gained the attention of scientists and engineers, given their advantages of uniform-sized spheroid generation and the ease with which the responses of individual spheroids can be monitored. Even though cost-effective methods such as the use of flexible membranes and ice lithography have been proposed, these techniques incur serious drawbacks such as difficulty in controlling the pattern sizes, achievement of high aspect ratios, and production of larger areas of microwells. To overcome these problems, we propose a robust method for fabricating concave microwells without the need for complex high-cost facilities. This method utilizes a 30 x 30 through-hole array, several hundred micrometer-order steel beads, and magnetic force to fabricate 900 microwells in a 3 cm x 3 cm polydimethylsiloxane (PDMS) substrate. To demonstrate the applicability of our method to cell biological applications, we cultured adipose stem cells for 3 days and successfully produced spheroids using our microwell platform. In addition, we performed a magnetostatic simulation to investigate the mechanism, whereby magnetic force was used to trap the steel beads in the through-holes. We believe that the proposed microwell fabrication method could be applied to many spheroid-based cellular studies such as drug screening, tissue regeneration, stem cell differentiation, and cancer metastasis.

Video Link

The video component of this article can be found at https://www.jove.com/video/55548/

Introduction

Cells grown into a spheroid form are more similar to real tissue in the body than a two-dimensional planar culture[1]. Given this advantage, the use of spheroids has been adopted to improve the study of cell to cell interaction[2,3], immune-activation[4], drug screening[5], and differentiation[6]. In addition, spheroids incorporating multiple cell types have recently been applied to organoids (near-physiological three-dimensional (3D) tissue), which are very useful for studying human development and disease[7]. Several methods have been used to produce spheroids. The simplest method involves the utilization of a non-adhesive surface, such that the cells aggregate with each other and form spheroids. A Petri dish can be treated with bovine serum albumin, pluronic F-127, or a hydrophobic polymer (e.g. poly 2-hydroxyethl methacrylate) to make its surface non-adhesive[8,9]. The spinner-flask method is another well-known means of producing large amounts of spheroids[10,11]. In this method, cells are held in suspension by stirring to prevent them from becoming attached to the substrate. Instead, the floating cells aggregate to form spheroids. Both the non-adhesive surface method and spinner flask method can produce large amounts of spheroids. However, they are subject to limitations including difficulties in controlling the spheroid size, as well as the tracking and monitoring of each spheroid. As a remedy for such problems, another spheroid production method, namely, the hanging drop method can be employed[12]. This involves depositing cell suspension drops onto the underside of the lid of a culture dish. These drops are usually 15 to 30 µL in size and contain approximately 300 to 3000 cells[13]. When the lid is inverted, the drops are held in place by surface tension. The microgravity environment in each drop concentrates the cells, which then form single spheroids at the free liquid-air interface. The benefits of the hanging drop method are that it offers a well-controlled size distribution, while it is easy to trace and monitor each spheroid, relative to the non-adhesive surface and spinner flask methods. However, this method incurs one disadvantage in that the massive production of spheroids and the production process itself is excessively labor intensive.

A microwell array is a flat plate with many micro-size wells, each having a diameter ranging from 100 to 1000 µm. The spheroid production principle when using microwells is similar to that of the non-adhesive surface method. Benefits include the fact that microwells provide spaces between the microwells for separating the cells or spheroids, such that it is easy to control the spheroid size, while also making it easy to monitor each single spheroid. With a large number of microwells, high-throughput spheroid production is also possible. Another advantage of microwells is the option to form wells of different shapes (hexahedral, cylindrical, trigonal prismatic) depending on the users' unique experimental purposes. Generally, however, a three-dimensional (3D) concave (or hemispherical) shape is regarded as being the most suitable for producing uniform-sized single spheroids. Therefore, the usefulness of concave microwells has been reported for many cell biology studies such as those

examining the cardiomyocyte differentiation of embryonic stem cells[14], the insulin secretion of islet cell clusters[15], the enzymatic activity of hepatocytes[16], and the drug resistance of tumor spheroids[17].

Unfortunately, the fabrication of microwells often requires specialized micropatterning facilities; conventional photolithography-based methods require exposure and developing facilities while reactive ion-etching-based methods need plasma and ion-beam equipment. Such equipment is costly which, together with the complicated fabrication process, presents a high barrier to entry for biologists who do not have access to microtechnology. To overcome these problems, other cost-effective methods such as ice lithography[18] (using frozen water droplets) and the flexible membrane method[14] (using a membrane, through-hole substrate, and a vacuum) have been suggested. However, these methods also incur serious drawbacks such as it being difficult to control the pattern sizes, the attainment of high aspect ratios, and the production of larger-area microwells.

To overcome the above issues, we are proposing a novel concave microwell fabrication method utilizing a through-hole substrate, steel beads, and a magnet array. Using this method, hundreds of concave spherical microwells can be fabricated by taking advantage of the mechanism of magnetic-force-assisted self-locking metallic beads (**Figure 1**). The fabrication process involves the use of very few expensive and complicated facilities and does not demand many advanced skills. As such, even unskilled persons can easily undertake this fabrication method. To demonstrate the proposed method, human-adipose-derived stem cells were cultured in the concave microwells to produce spheroids.

Protocol

1. Preparation of through-hole array aluminum plate and magnet array

1. Prepare two 50 mm x 50 mm (or larger) aluminum plates. The thickness of each plate was 300 µm that is half of the bead diameter.
2. Form a 30 x 30 through-hole array on one of the aluminum plates by using a CNC rotary engraver with a Φ550-µm micro drill bit with 30 mm/s of plunge rate and 8000 RPM of spindle speed. The distance between each hole (center to center) was 1 mm (**Figure 1a** and **Figure 2a**, **i**).
3. Form a 30 x 30 array of Φ750-µm through-holes on the other aluminum plate, using the same procedure as that described in 1.2 (**Figure 1a** and **Figure 2a**, **ii**).
4. Attach the two plates each other by using a sticky tape and form Φ3 mm alignment holes at each of the four corners of both aluminum plates.
5. Soak the aluminum plates in 15% sulfuric acid for 12 h to clean their surfaces. Since the thin layer of aluminum oxide on the surface of the aluminum make it corrosion resistant, the hole diameter and thickness of the plate are not changed by this acid treatment.
6. Form a 30 × 30 array of 1 x 1 x 1 mm neodymium magnets (with a magnetic strength of 0.363 N). Ensure that each magnet is the opposite polarity to its neighbor. To prevent the breaking or scattering of the magnet array, attach a 30 x 30 mm aluminum plate to the bottom of the magnet array using double-sided tape (**Figure 2a**, **iii and inset in Figure 2**).

2. Bead trapping process

1. Align and stack the two aluminum plates (top plate: 750-µm-hole plate, bottom plate: 550-µm-hole plate) using the prepared alignment holes at the four corners of each plate (**Figure 1b**).
2. Lock the two plates together by inserting M3 bolts into the alignment holes, and then secure the bolts with nuts (**Figure 1b**).
3. Stack the aluminum plate assembly on the prepared magnet array (**Figure 1b**, **2b**, and **2c**). Align the array of magnets and the array of through holes in the aluminum plate during the stacking process. Then use a sticky tape to fix the position of the magnet array.
4. Place a sufficient number of Φ600 mm SUJ2 steel beads on the plate assembly and manipulate the beads using an acryl (or non-metallic) plate such that a bead becomes trapped in each hole (**Figure 1c**, **1d**, and **1e**) while simultaneously removing the excess beads which have not lodged in the holes.
5. Carefully remove the top plate to avoid unwanted scattering and dislocation of the trapped beads (**Figure 1f**).

3. Concave microwell fabrication

1. Move the concave microwell mold, produced in steps 2.1 to 2.5, above, to a Petri dish.
2. Mix polydimethylsiloxane (PDMS) monomer and curing agent according to the manufacturer's instructions[19] with a PDMS monomer:curing agent ratio of 10:1.
3. De-gas the PDMS mixture by using a desiccator and vacuum pump to remove any bubbles trapped in the PDMS mixture.
4. Pour the PDMS mixture into the concave microwell mold and de-gas again using the same procedure as that described in 3.3 (**Figure 1f**).
5. Bake the PDMS mixture on a hotplate at 80 °C for 2 h to form a bead-embedded PDMS substrate (**Figure 1g**).
6. Remove the cured PDMS substrate from the mold (**Figure 1g**). In the removing process, spray methanol using washing bottle to detach PDMS substrate from the mold.
7. Using a Φ15 mm x 2 mm magnet, remove the trapped steel beads from the PDMS substrate (**Figure 1h**). For this process, any magnet that is sufficiently strong to extract the beads from the PDMS substrate can be used.

4. Spheroid culture

1. Cut the concave microwell-patterned PDMS substrate by using a Φ14 mm biopsy punch to be fitted in 24-well plate in this study.
2. Sterilize the resulting Φ14 mm PDMS substrate in an autoclave sterilizer at 121 °C and 15 psi.
3. Place the sterilized PDMS substrate into a 24 well plate.
4. Coat the entire PDMS substrate with 4% (w/v) pluronic F-127 solution overnight to prevent cell attachment to the microwell surface. During the coating process, remove any air bubbles entrapped in the concave microwells by pipetting or by using an ultrasonic cleaner.
5. Flush the F-127 solution three times by using phosphate-buffered saline (PBS).

6. Seed 1 mL of cell-medium (Dulbecco's Modified Eagle Medium) solution (which contains 2 x 10^6 cells) on the PDMS substrate. Note that the seeding density can be changed according to the target spheroid size and/or target cell type. Here, adipose-derived stem cells (ASC) were used.
7. Aspirate the 1 mL of medium using a 1000 µL pipette to remove any excess cells that were not trapped in the microwells (**Figure 3**).
8. Incubate the cells at 36.5 °C, humidity of >95%, and 5% CO_2 condition. In the case of the ASCs used in our study, the cells aggregate to a spheroid in 48 h.

Representative Results

A convex mold and microwell pattern were successfully fabricated by following steps 2.1 to 3.7. (**Figure 4**). The commercial steel beads were trapped in the 30 x 30 through-hole array. The beads were held tightly without any gaps between the beads and the corresponding through-holes (**Figure 4a**). The shape of fabricated concave microwell is concave hemispherical, with a diameter of 600 µm, which is the same as that of the steel bead (**Figure 4b**). A cross-section of a concave microwell (**Figure 4c**) shows that the distance from the neighboring microwell was 1 mm (center to center), which was the same as that of the through-holes. The Φ14 mm concave microwell substrate, which was placed in the 24 well plate, contained over 120 microwells (**Figure 4d**).

Adipose-derived stem cells were cultured in the concave microwells. We seeded 2 x 10^6 cells on the Φ14 mm concave microwell array. After 24 h, the cells had aggregated into spheroids, as shown in **Figure 4**. The average diameter of the spheroids formed in our microwell array was 185.68 ± 22.82 µm (day 1, **Figure 5a**, **5c**). At day 3, the cells had become more aggregated, with the average diameter of the spheroids falling to 147.00 ± 17.11 µm (**Figure 5b**, **5d**).
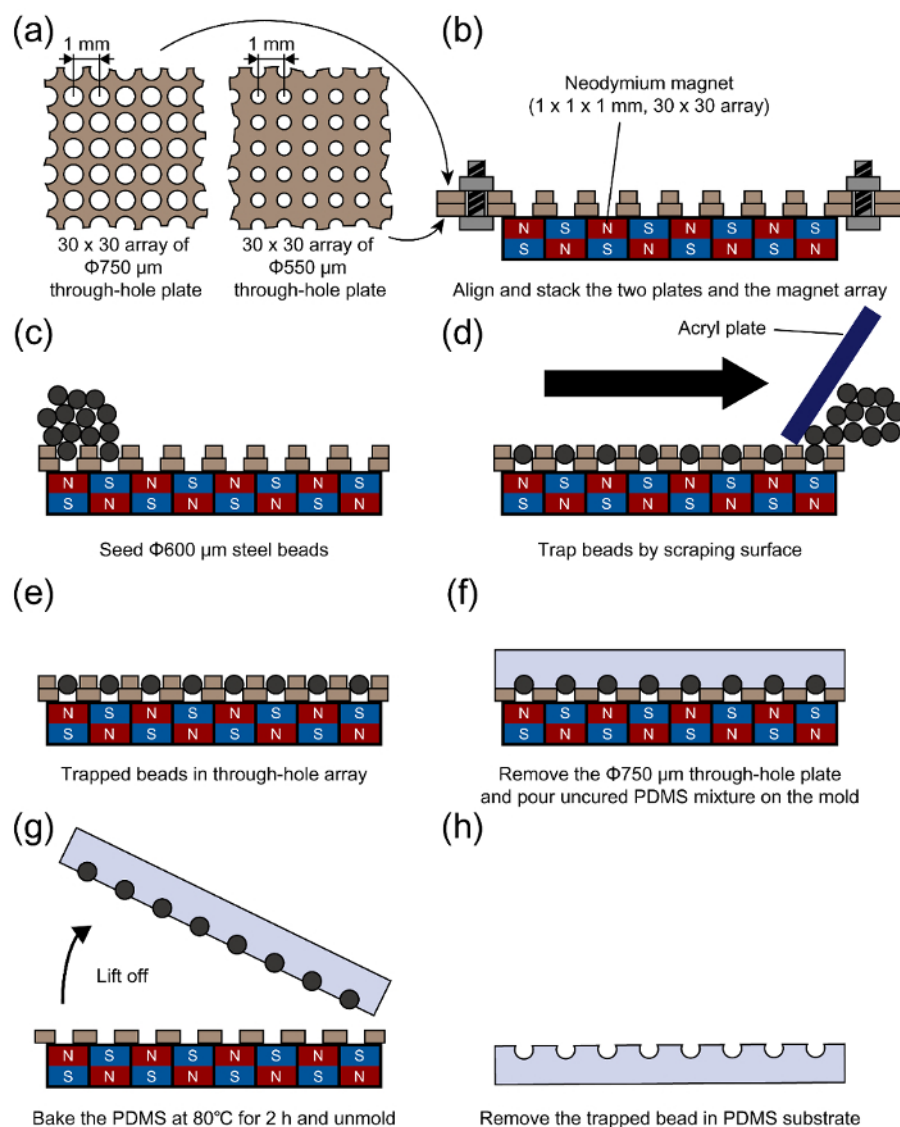
Figure 1: Schematic of fabrication process. (a) Making 30 x 30 Φ550 and 750 µm through-hole array in aluminum plates using CNC engraver. (b) Aligning the two through plates by using the alignment holes. Subsequently, the aligned plates were stacked on the magnet array. (c) Seeding a sufficient amount of steel beads onto the plates. (d) Scraping the beads using an acryl plate to trap the beads in the through-hole array. (e) Beads were trapped in the through-hole array. (f) The top plate (Φ750-µm through-hole array) was removed and uncured PDMS mixture was poured into the mold. (g) After the PDMS was baked at 80 °C for 2 h, the cured PDMS was unmolded. (h) The cured PDMS grabs the steel beads. The beads are then removed using a neodymium magnet (Φ15 mm with a thickness of 2 mm). Please click here to view a larger version of this figure.
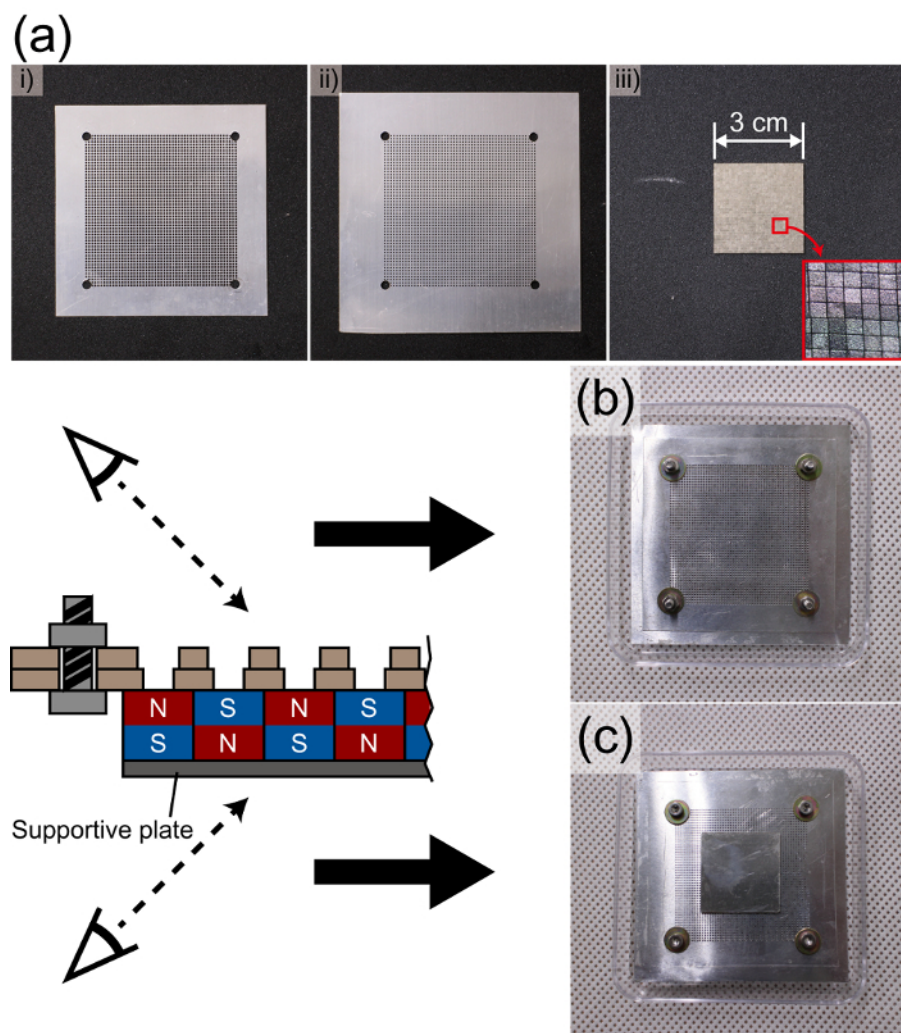
Figure 2: Fabrication process. (a) Preparing two through-hole plates and magnet array. i) Aluminum plate having 750 µm through-hole array. ii) Aluminum plate having 550 µm through-hole array. iii) 30 x 30 array of 1 mm x 1 mm x 1 mm magnets. (b) Top view of stacked and aligned plates. (c) Bottom view of stacked and aligned plates and magnet array. Please click here to view a larger version of this figure.
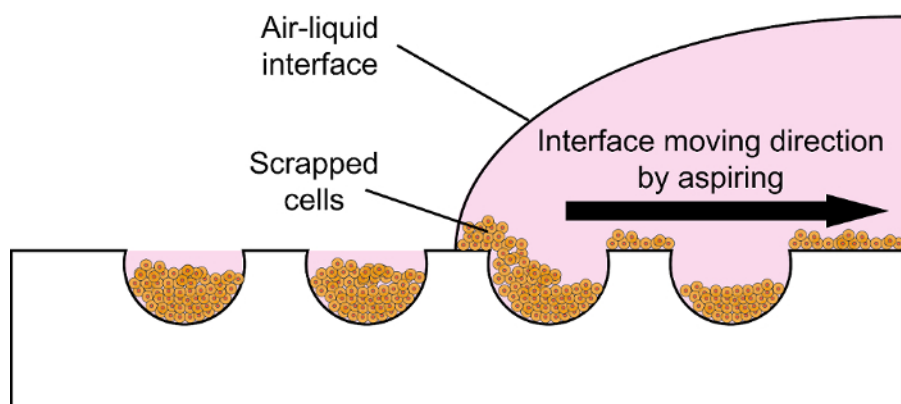

Figure 3: Removing excessive cells by receding meniscus. By aspiring the medium, the surface tension was caused by air-liquid interface, then the surface tension scrapped excessive cells on surface of microwell substrate. Please click here to view a larger version of this figure.
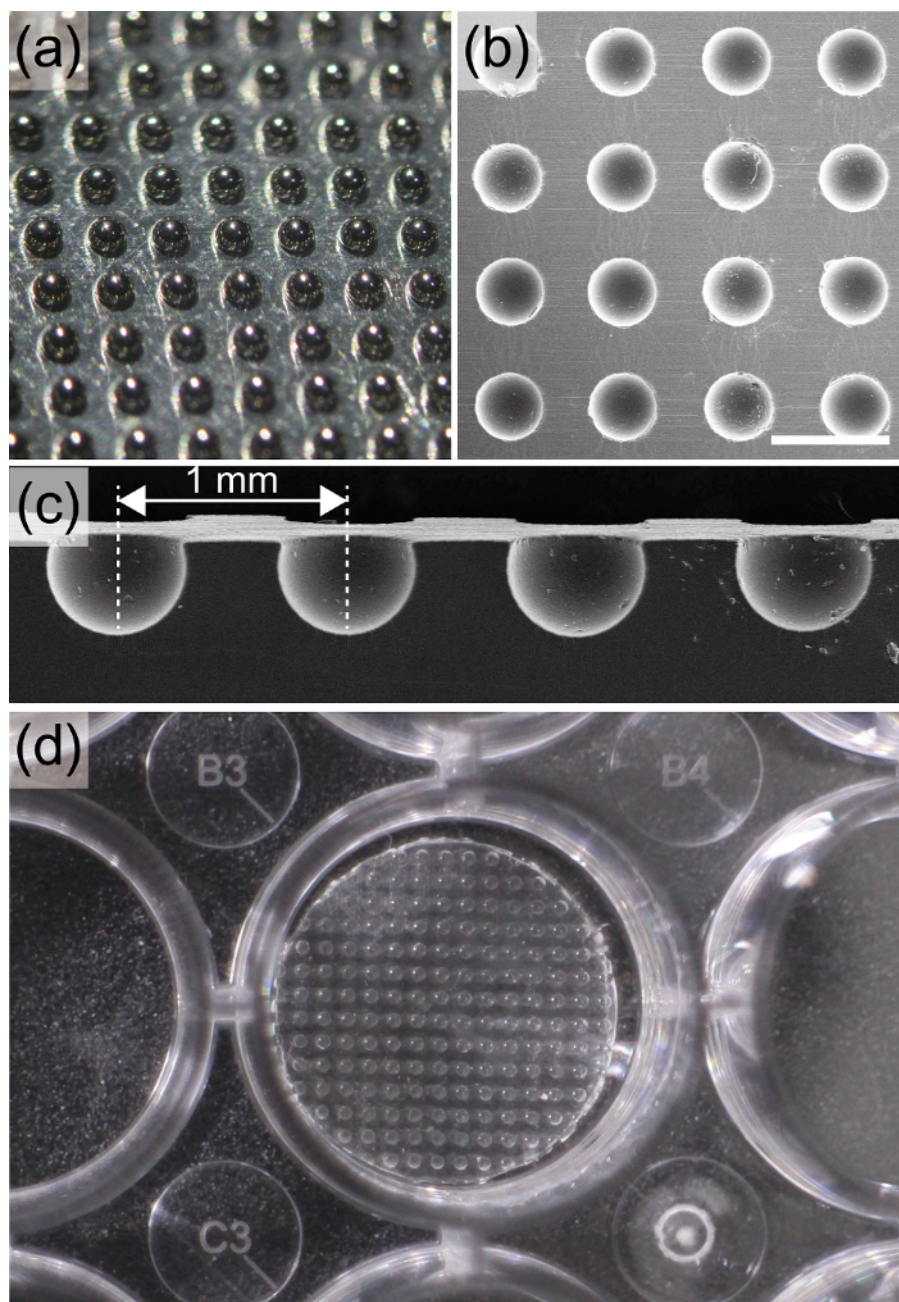
Figure 4: Convex mold and fabricated microwell array. (a) Trapped beads in through-hole array aluminum plate. The trapped beads act as a mold to fabricate the concave microwells. The bead size was 600 µm. The scale bar is 1 mm. (b) and (c) SEM images of fabricated microwells. Each fabricated microwell has a hemispherical shape, 600 µm in diameter. (d) Φ14-mm microwell array in 24-well plate. The array contains over 120 concave microwells. Please click here to view a larger version of this figure.
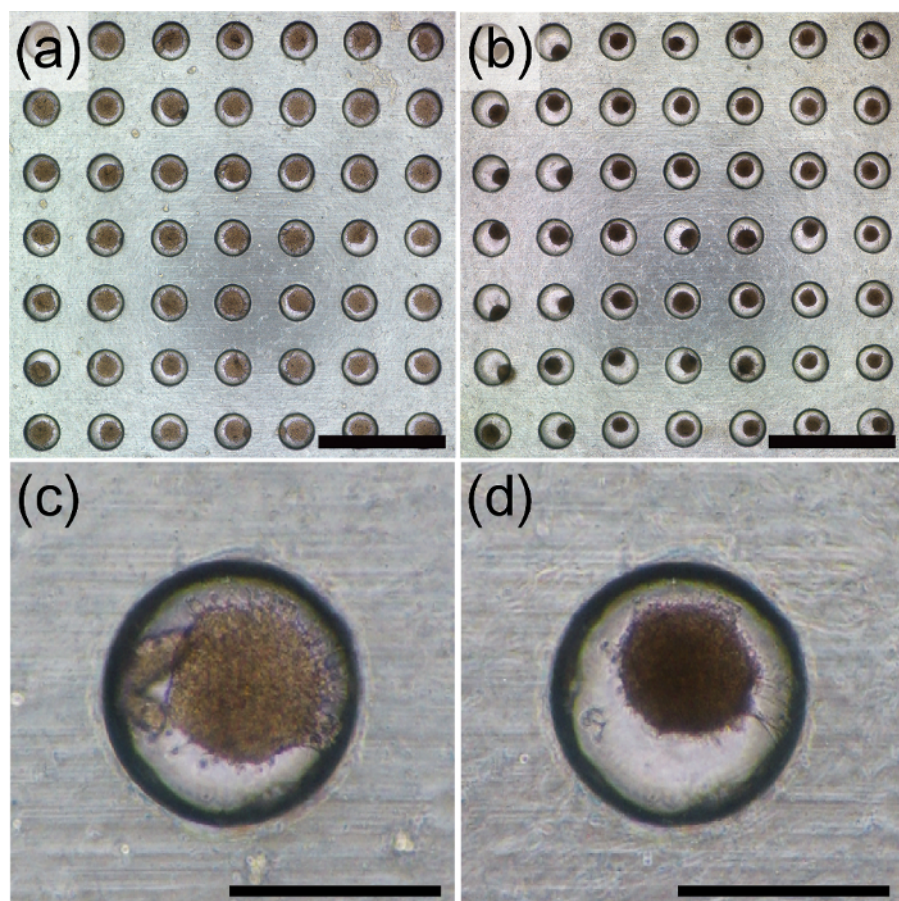
Figure 5: Culture spheroids in concave microwell array. The Φ14-mm microwell array was seeded with 2 x 10⁶ ASCs and cultured for 3 days. (a) Cultured spheroids at Day 1; the cells have started to form spheroids. The scale bar is 2 mm. (b) Cultured spheroids at Day 3; the formed spheroids are more tightly structured, while their average diameter has fallen from 185.68 ± 22.82 µm at Day 1 to 147.00 ± 17.11 µm at Day 3. The scale bar is 2 mm. (c) Magnification images of spheroid at Day 1. The scale bar is 500 µm. (d) Magnification images of spheroid at Day 3. The scale bar is 500 µm. Please click here to view a larger version of this figure.
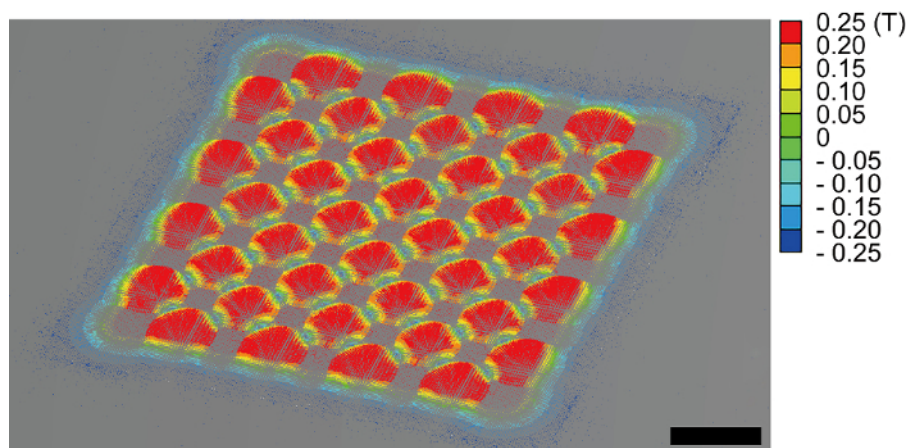

Figure 6: Simulation result for vector of magnetic flux density. The density of the magnetic flux on the magnet array was computed using the magnetostatic module. The simulation result shows that the strongest magnetic flux density is at center of each magnet, causing the beads to be trapped in the center of the through-holes where they became securely fixed. The scale bar is 2 mm. Please click here to view a larger version of this figure.
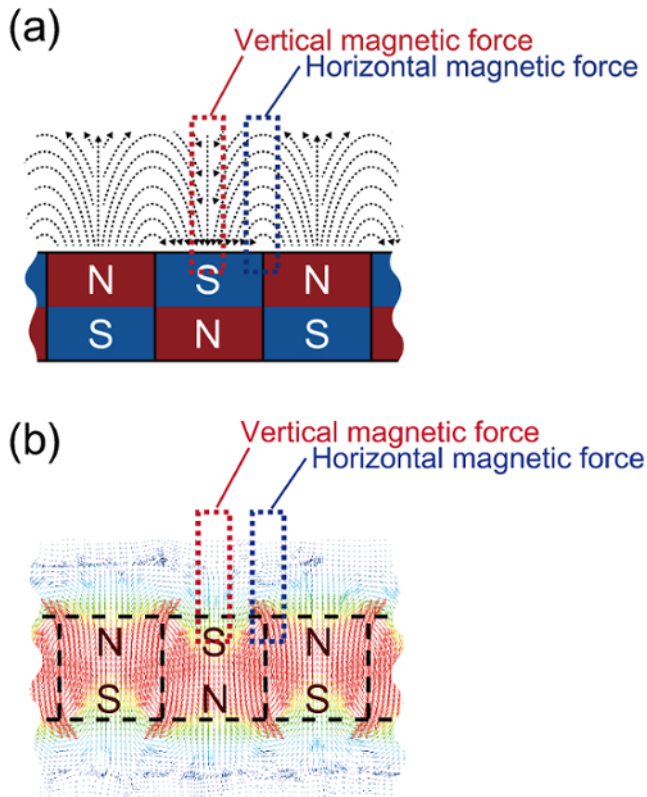
Figure 7: Magnetic field distribution of magnet array. Each magnet is of the opposite polarity to its neighbor. The horizontal magnetic field is dominant at the interface between neighboring magnets, while the vertical magnetic field is strongest at the center of each magnet. These directional forces guide a bead to the center of a magnet. (a) Magnetic field of magnet array. (b) Vector of magnetic field as determined by magnetostatic simulation. Please click here to view a larger version of this figure.
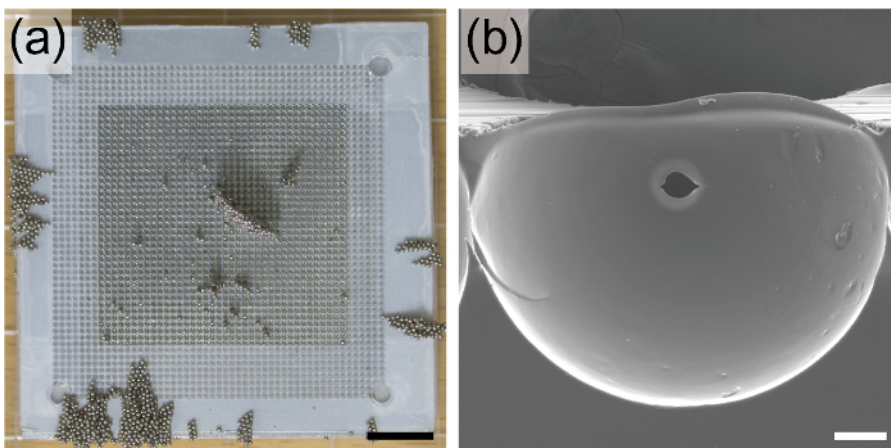
Figure 8: Limitation using single big magnet and of bead size. (a) Unlike the case of using an array of small magnets, when one large magnet is used, almost all of the beads tend to move to the edge or center of the magnet where the high density magnetic field is formed. Further, the beads are connected to form a chain shape. The scale bar is 10 mm. (b) SEM image of linked microwell which was fabricated by using Φ800 μm beads with 1 mm x 1 mm x 1 mm magnet array. Using a bead that is too large in size relative to the size of the magnet can create a small hole in the wall between adjacent microwells. The scale bar is 100 μm. Please click here to view a larger version of this figure.
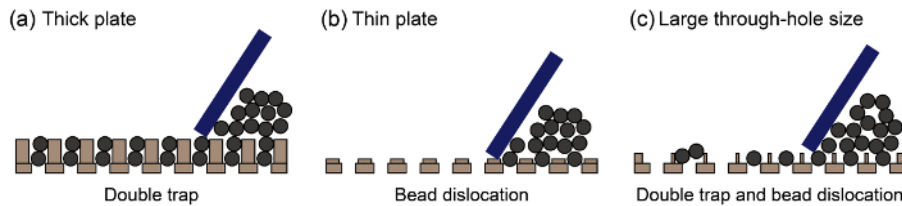
Figure 9: The importance of choosing the appropriate top plate thickness and hole size in the bead trapping process. (a) If the top plate is too thick, a double trap will occur. (b) Conversely, if the top plate is too thin, there is a tendency for the beads to come off. (c) If the size of the through-hole is larger than the bead diameter, both double trap and bead dislocation may occur. Please click here to view a larger version of this figure.

Discussion

The major challenge facing this fabrication method was the secure fixing of the beads in the through-hole array in the aluminum plate. To solve this challenge, magnetic force in the form of a 30 x 30 magnet array was used to fix the beads securely, as shown in **Figures 6** and **7**. The magnetic flux density of the magnet array, which has the opposite polarity, is strongest at the center of each magnet surface. Because the strength of the magnetic force depends on the flux density, the beads were guided to the center of the top surface of each magnet where they were held in position. If a single large-sized magnet (5 cm × 5 cm × 1 cm) was used, the beads, especially the ones located in the extreme outside holes, tend to be attracted to the higher intensity magnetic field created at the magnet edge. Another problem with using large magnets is that the beads stick together spontaneously to create small bead chains (**Figure 8a**).

The role of top plate (750 μm hole) was to serve the pit geometry to trap beads. Due to this pit structure, it is possible to scratch the beads with an acrylic plate to create a large number of trapped bead arrays at once (protocol 2.4 and **Figure 1c** and **1d**). If not using the top plate, each bead must be manually inserted into the base (550 μm hole) one at a time.

The limitations of our method include the need for a CNC engraver that is the most expensive device used in the method. Such CNC machines are priced from around $3000. This, however, is still much cheaper than conventional soft lithography facilities. Another inherent limitation of our method is the need for small magnets, and the gap between the microwells is dependent on the magnet size, which was 1 mm in the demonstration described in this paper. It would be difficult to reduce this gap much more since magnets smaller than 500 μm are not readily available. In addition, maximum size of bead was also limited. The trapped beads were magnetized by magnets. If the gap between magnetic beads were too narrow, the probability of sticking together is higher than some of the microwells were connected by holes as shown in **Figure 8b**. Therefore, when 1 mm x 1 mm x 1 mm magnets are used, beads with a diameter of 700 μm or more are not recommended

Compared with other fabrication methods such as flexible membrane[14], ice lithography[18] and deep reactive ion etching[20], this fabrication method does not require special lithography facilities, allows the microwell position to be easily controlled, and can produce a standardized concave microwell shape. In addition, wet etching of PDMS[21], grayscale lithography[22], and backside diffused light lithography[23] have been proposed for the production of concave geometries. However, wet etching of PDMS requires a rectangular structure first to make a concave and round microwell, and is not suitable for making an open microwell. The greyscale lithography method has the advantage of utilizing existing photo lithography facilities, but the need of high priced facilities and greyscale photo mask is a disadvantage. Backside diffused light lithography was another recently reported method useful to fabricate concave microwells with various aspect ratios, but only at the low resolution of pattern density.

The critical step in the concave microwell fabrication is the selection of the thickness of the and the through-hole size of top plate (step 1.1 and 1.3). If the through-hole plate is too thick, multiple beads can be trapped in each through-hole (**Figure 9a**); if it is too thin, the beads will not be fixed in step 2.4 and thus dislocated from the through-holes (**Figure 9b**). In case of the larger through-hole, both multiple trap and dislocation can occur (**Figure 9c**).

As a guideline for selecting the size of the magnet and the thickness of the through-hole plate, it is recommended that the size of the magnet and the thickness of the "through-hole plate" be based on the size of the bead. The size of the magnet must be larger than the diameter of the bead, and the thickness of the through-hole plate should not exceed the diameter of the bead. However, since the choice of magnets and plate thickness is empirical, more detailed optimization and parametric studies will be included in future studies.

Future goals of our method include the fabrication of stem cell niche-like microwells for biomimetic in vitro hair follicles[24], customized microwells for organoid generation[25], and diverse arrays of different-sized microwells for studying the dependence of cancer cells and immune cells on spheroid size.

Disclosures

The authors have no conflicts of interest to disclose.

Acknowledgements

References

1. Fennema, E., Rivron, N., Rouwkema, J., van Blitterswijk, C., & de Boer, J. Spheroid culture as a tool for creating 3D complex tissues. *Trends Biotechnol.* **31** (2), 108-115 (2013).
2. Djordjevic, B., & Lange, C. S. Hybrid spheroids as a tool for prediction of radiosensitivity in tumor therapy. *Indian J Exp Biol.* **42** (5), 443-447 (2004).
3. Takezawa, T., Yamazaki, M., Mori, Y., Yonaha, T., & Yoshizato, K. Morphological and immuno-cytochemical characterization of a hetero-spheroid composed of fibroblasts and hepatocytes. *J Cell Sci.* **101** (3), 495-501 (1992).
4. Gottfried, E., Kunz-Schughart, L. A., Andreesen, R., & Kreutz, M. Brave little world: spheroids as an in vitro model to study tumor-immune-cell interactions. *Cell Cycle.* **5** (7), 691-695 (2006).
5. Zhang, X. *et al.* Development of an in vitro multicellular tumor spheroid model using microencapsulation and its application in anticancer drug screening and testing. *Biotechnol Prog.* **21** (4), 1289-1296 (2005).
6. Kim, B.-C. *et al.* Microwell-mediated micro cartilage-like tissue formation of adipose-derived stem cell. *Macromol Res .* **22** (3), 287-296 (2014).
7. Fatehullah, A., Tan, S. H., & Barker, N. Organoids as an in vitro model of human development and disease. *Nature cell biology.* **18** (3), 246-254 (2016).
8. Yuhas, J. M., Li, A. P., Martinez, A. O., & Ladman, A. J. A simplified method for production and growth of multicellular tumor spheroids. *Cancer Res.* **37** (10), 3639-3643 (1977).
9. Hamilton, G. A., Westmoreland, C., & George, E. Effects of medium composition on the morphology and function of rat hepatocytes cultured as spheroids and monolayers. *In Vitro Cell Dev Biol-Animal.* **37** (10), 656-667 (2001).
10. Nyberg, S. L. *et al.* Rapid, large-scale formation of porcine hepatocyte spheroids in a novel spheroid reservoir bioartificial liver. *Liver Transplant.* **11** (8), 901-910 (2005).
11. Lazar, A. *et al.* Extended liver-specific functions of porcine hepatocyte spheroids entrapped in collagen gel. *In Vitro Cell Dev Biol-Animal.* **31** (5), 340-346 (1995).
12. Kelm, J. M., Timmins, N. E., Brown, C. J., Fussenegger, M., & Nielsen, L. K. Method for generation of homogeneous multicellular tumor spheroids applicable to a wide variety of cell types. *Biotechnol Bioeng.* **83** (2), 173-180 (2003).
13. Lin, R. Z., & Chang, H. Y. Recent advances in three-dimensional multicellular spheroid culture for biomedical research. *Biotechnol J .* **3** (9-10), 1172-1184 (2008).
14. Choi, Y. Y. *et al.* Controlled-size embryoid body formation in concave microwell arrays. *Biomaterials.* **31** (15), 4296-4303 (2010).
15. Hwang, J. W. *et al.* Functional clustering of pancreatic islet cells using concave microwell array. *Macromol Res .* **19** (12), 1320-1326 (2011).
16. Wong, S. F. *et al.* Concave microwell based size-controllable hepatosphere as a three-dimensional liver tissue model. *Biomaterials.* **32** (32), 8087-8096 (2011).
17. Yeon, S.-E. *et al.* Application of concave microwells to pancreatic tumor spheroids enabling anticancer drug evaluation in a clinically relevant drug resistance model. *PloS one.* **8** (9), e73345 (2013).
18. Park, J. Y., Hwang, C. M., & Lee, S.-H. Ice-lithographic fabrication of concave microwells and a microfluidic network. *Biomed Microdevices.* **11** (1), 129-133 (2009).
19. Corning, D. Sylgard 184 Silicone Elastomer. *Technical Data Sheet.* (2008).
20. Giang, U.-B. T., Lee, D., King, M. R., & DeLouise, L. A. Microfabrication of cavities in polydimethylsiloxane using DRIE silicon molds. *Lab on a Chip.* **7** (12), 1660-1662 (2007).
21. Choi, J. S. *et al.* Capture and culturing of single microalgae cells, and retrieval of colonies using a perforated hemispherical microwell structure. *RSC Advances.* **4** (106), 61298-61304 (2014).
22. Zhong, K., Gao, Y., Li, F., Zhang, Z., & Luo, N. Fabrication of PDMS microlens array by digital maskless grayscale lithography and replica molding technique. *Optik .* **125** (10), 2413-2416 (2014).
23. Lai, D. *et al.* Simple multi-level microchannel fabrication by pseudo-grayscale backside diffused light lithography. *RSC advances.* **3** (42), 19467-19473 (2013).
24. Pan, J. *et al.* Fabrication of a 3D hair follicle-like hydrogel by soft lithography. *J Biomed MAter Res A.* **101** (11), 3159-3169 (2013).
25. Mori, R., Sakai, Y., & Nakazawa, K. Micropatterned organoid culture of rat hepatocytes and HepG2 cells. *J Biosci Bioeng.* **106** (3), 237-242 (2008).